RSC Advances

PAPER

View Article Online
View Journal | View Issue

Cite this: *RSC Adv.*, 2014, **4**, 5698

Magnetite as a heterogeneous electro Fenton catalyst for the removal of Rhodamine B from aqueous solution†

P. V. Nidheesh,[a] R. Gandhimathi,*[a] S. Velmathi[b] and N. S. Sanjini[b]

Received 23rd November 2013
Accepted 11th December 2013

DOI: 10.1039/c3ra46969g

www.rsc.org/advances

This paper deals with the investigation of Rhodamine B (RhB) dye removal characteristics of the heterogeneous electro Fenton (EF) process using laboratory prepared Fe_3O_4. Throughout the experiment graphite–graphite electrolytic systems with the electrodes having a surface area of 25 cm^2 were used. Removal efficiencies of Fe_3O_4 prepared at various Fe^{2+} : Fe^{3+} ratios were found to be close to the same range and Fe_3O_4 with 2 : 1 ratio was selected for further experiments. The effects of solution pH, catalyst concentration, voltage, electrode spacing *etc.* on dye removal efficiency were analysed to determine the optimal operating conditions. The experiment results indicated that 97.3% of RhB was removed within 180 min of electrolysis from a solution containing 10 mg l^{-1} of RhB at pH 3 with a catalyst concentration of 10 mg l^{-1}, an applied voltage of 8 V and an inner electrode spacing of 4 cm. It was also found that addition of anions negatively affected the efficiency of the electrolytic system and followed the order $CO_3^{2-} \sim Cl^- > SO_4^{2-} > NO_3^- > HCO_3^-$. The reusability of magnetite highlights the practical applicability of heterogeneous EF process over homogeneous EF processes. Also, compared to the Fenton process, the optimal catalyst concentration required for the EF process was much less. From the present study, it can be concluded that heterogeneous EF process using Fe_3O_4 is an alternative method for dye removal from aqueous solution.

A. Introduction

Advanced oxidation processes (AOPs) based on highly reactive hydroxyl radicals for wastewater purification have received great attention in recent years.[1–5] The hydroxyl radical (2.8 V) is the most powerful oxidizing reagent after fluorine (3.06 V).[6] This radical reacts with organic pollutants until the mineralization of compounds, results in water, carbon dioxide and inorganic ions in the aqueous medium.[7] Among AOPs, electrochemical advanced oxidation processes (EAOPs) like anodic oxidation and indirect electro-oxidation methods based on H_2O_2 electro-generation are very attractive for wastewater decontamination. This is due to their low cost and high effectiveness of persistent organic pollutants (POPs) removal, without needing the addition of toxic chemical reagents and producing hazardous wastes.[8,9] Among these, Fenton based EAOPs, known as electro Fenton (EF) process is a popular and efficient method. These processes involve the continuous supply of H_2O_2 from the cathode surface to an acidic solution from the two electron reduction of O_2 gas as in eqn (1).[3] The *in situ* produced H_2O_2 further undergoes conventional Fenton process as in eqn (2). The hydroxyl radicals produced from the Fenton process then react with POPs resulting to its degradation and mineralization. One of the main advantages of EF process is the insignificant change of solution pH during electrolysis and fast degradation of pollutants.[1–3,10] The protons consumed at the cathode during the conventional Fenton process are balanced by the water oxidation reaction at the anode as in eqn (3).[10] EF process rectifies the main drawbacks of Fenton process by the *in situ* production of H_2O_2 and removal or degradation of pollutants without sludge production. Electroregeneration of ferrous ions from ferric ions is another advantage of EF process. Ferric ions produced *via* conventional Fenton reaction are reduced to ferrous ions at the cathode as in eqn (4).[11] EF process has been used for the removal and degradation of various pollutants such as dyes,[8,12,13] paper pulp treatment effluents,[14] diuron,[15] dephalexin,[16] organics in reverse osmosis concentrate,[17] chlorophenol,[18] landfill leachate[19] *etc.*

$$O_2 + 2H^+ + 2e^- \rightarrow H_2O_2 \quad (1)$$

$$Fe^{2+} + H_2O_2 \rightarrow Fe^{3+} + OH^- + HO^{\cdot} \quad (2)$$

$$H_2O \leftrightarrow 1/2O_2 + 2H^+ + 2e^- \quad (3)$$

[a]*Department of Civil Engineering, National Institute of Technology, Tiruchirappalli – 620 015, Tamil Nadu, India. E-mail: rgmathii@nitt.edu; Fax: +91 431 250 0133; Tel: +91 431 250 3171*

[b]*Department of Chemistry, National Institute of Technology, Tiruchirappalli – 620 015, Tamil Nadu, India*

† Electronic supplementary information (ESI) available. See DOI: 10.1039/c3ra46969g

$$Fe^{3+} + e^- \rightarrow Fe^{2+} \quad (4)$$

Recently, wastewater treatment using Fe_3O_4 magnetic nanoparticles has attracted significant interest. Peroxidase activity of Fe_3O_4 nanoparticles combined with its unique characteristic, such as easy preparation, high stability and convenient separation from solution by external magnetic field, provides a promising method to remove phenolic and aniline compounds from wastewater.[20] Absalan *et al.*[21] used nanoparticles of Fe_3O_4 for the efficient removal of reactive red 120 from aqueous solution. Fe_3O_4-multi-walled carbon nanotubes also found as an efficient Fenton like catalyst for the decomposition of dyes from aqueous solution.[22] Recently, the efficiency of composite materials containing magnetite also tested as heterogeneous Fenton reagents by various researchers. Degradation of 4-chlorophenol by Fe_3O_4/CeO_2 has been studied by Xu and Wang[23] and reported that addition of CeO_2 enhanced the activity of magnetite. Humic acid coated Fe_3O_4 magnetic nanoparticles exhibited high activity to produce hydroxyl radicals through catalytic decomposition of H_2O_2 and most sulfathiazole was degraded within 1 h, and >90% of total organic carbon were removed during the reaction period of 6 h.[24] Magnetite-loaded mesocellular carbonaceous material exhibited superior activity as a heterogeneous Fenton catalyst and an adsorbent for removal of phenol and arsenic from aqueous solution.[25] Similarly, the presence of titanium and vanadium in magnetite greatly improved the catalytic activity of natural magnetite for the Acid Orange II decolorization.[26]

The present study analyzes the efficiency of laboratory prepared Fe_3O_4 by chemical precipitation method, as a heterogeneous electro Fenton catalyst for the removal of Xanthene dye, Rhodamine B (RhB) from aqueous solution. The influence of several operational parameters such as solution pH, initial dye concentration, Fe_3O_4 concentration, voltage *etc.* on RhB removal efficiency of the heterogeneous EF process is also investigated.

B. Experimental

Chemicals

AR grade chemicals: $FeSO_4 \cdot 7H_2O$, $FeCl_3$, Na_2SO_4, NaCl, Na_2CO_3, $NaHCO_3$, NaOH, $NaNO_3$ and H_2SO_4 from Merck was used for all the electrolytic experiments and preparation of Fe_3O_4. RhB dye stuff supplied by Loba Chemie, was used without further purification in all the experiments. A stock solution of RhB having concentration of 1 g l^{-1} was prepared by dissolving 1 g of dye stuff in 1000 ml of distilled water and stored in a dark place. Required quantity of working solution was prepared by diluting the above stock solution in distilled water.

Electrodes

Graphite plates of size 24 × 14 cm from Anabond Sainergy Fuel Cell India Private Limited, Chennai, Tamil Nadu, India were used as electrode material. The plates were cut into pieces having an area of 25 cm^2 and were used as both cathode and anode.

Preparation and characterization of Fe_3O_4

Fe_3O_4 was prepared in the laboratory by the chemical precipitation method. The ideal chemical reaction of Fe_3O_4 precipitation is given in eqn (5).[27] 100 ml solution containing Fe^{2+} and Fe^{3+} in different molar ratios was prepared using distilled water. The initial pH values of ferrous and ferric ion solutions were found as 3 and 2 respectively. These solutions were mixed together in a conical flask and were agitated using an orbital shaker in a vigorous manner. The pH of the mixed solution after shaking was observed as 2.5. The spectral and color changes of these solutions are shown in Fig. S1 and S2,† respectively. To this solution, 8 to 10 ml of 8 M NaOH was added slowly until the formation of black precipitate (Fe_3O_4). The final pH of the solution after the formation of Fe_3O_4 was noted as 12.5. The agitation was continued up to half an hour. This precipitate was filtered and washed several times using distilled water. Then the precipitate was kept in an oven at 75 °C for 24 h and used for experiments without further purification.

$$Fe^{2+} + 2Fe^{3+} + 8OH^- \rightarrow Fe_3O_4 \text{ (black colloidal particles)} + 4H_2O \quad (5)$$

Scanning electron microscopy (SEM) investigations of the magnetite samples were conducted in a JEOL JMT-300 operated at 15 kV. The surface functional groups of magnetite were detected by Fourier Transform Infrared (FTIR) Spectroscopy (FTIR-2000, Perkin Elmer) using KBr pellet method. The spectra were recorded from 4000 to 400 cm^{-1}. The X-ray diffraction (XRD) spectrum of magnetite was obtained at a scan rate of 4° min^{-1} by using a Rigaku X-ray Diffractometer (D-Max/Ultima III). The prepared magnetite sample was exposed to X-ray with the 2θ angle varying between 10° and 80° with Cu Kα radiations at an applied voltage and current of 40 kV and 30 mA, respectively. The UV-Vis diffuse reflectance was measured in the samples at room temperature in air on a Shimadzu UV-2600 UV-Visible spectrophotometer.

Experimental procedure

Batch electrolytic experiments for 10 mg l^{-1} of RhB solution at acidic conditions was carried out in a 1000 ml cylindrical beaker. 750 ml of the solution was considered as the working volume for the electrolysis experiments. The initial pH of the dye solution was adjusted to 3 (in most of the experiments) using 0.5 N H_2SO_4 and monitored using Orion EA 940 expandable ion Analyzer (Thermo Electron Corporation, USA). Graphite plates of effective area 25 cm^2 were used as the both electrodes. The electrodes were placed inside the reactor vertically and adjusted to required inner electrode spacing. Required amount of Fe_3O_4 was added to this solution and mixed well. Before the electrolysis of the solution, air was purged into it using commercially available 'fish aerator' and continues till the experiments ends. Homogeneous mixing and saturation of oxygen in the solution is fulfilled with this aeration process. After 10 min of aeration, electrolysis experiments were started at constant voltage. DC power supply (Make: Beetech) was used for supplying constant voltage across the graphite plates. During the electrolysis, samples were collected at various time intervals

and residual concentration of RhB was measured using UV/Vis spectrophotometer (Lambda 25, Perkin Elmer, USA) at 553.8 nm. All the experiments were conducted at room temperature for 180 min. For the preliminary electrolysis, 10 mg l^{-1} of RhB solution, solution pH of 3, applied voltage of 8 V, inner electrode spacing of 4 cm, electrode area 25 cm^2 and magnetite concentration of 10 mg l^{-1} were considered. Effects of various key operational parameters on RhB removal was studied by varying the specific parameter without varying other parameters.

Recycling of magnetite

Reusability of material is one of the main advantages of heterogeneous catalyst over homogeneous catalysts. After each electrolytic experiment, the magnetite particles were filtered from the solution and dried in oven at 75 °C for 24 h. This catalyst was used for the oxidation of RhB solution and experiment was carried out at the identical conditions for which experiments carried out for the raw magnetite particles.

Metal leaching study

Leaching of Fe ions from the magnetite surface was monitored during the electrolysis. The concentration of ferrous ions in the electrolyte was measured as per modified 1,10-phenanthroline method.[28] To a 15 ml of sample, 1 ml of 1 : 4 (v/v) sulphuric acid, 2 ml of 2 M sodium fluoride, 2 ml of 1,10-phenanthroline and 3 ml of 3 M hexamethylenetetramine solutions were added sequentially. After mixing well, the final volume of the solution was made upto 25 ml using distilled water. Peak at 510 nm was observed for this solution as in Fig. S3.† Then the instrument was calibrated at this peak using various concentrations of ferrous solution. The actual ferrous concentration in the electrolysed RhB solution was calculated from the calibration graph after the blank correction as in eqn (6).

$$A = A_1 - A_2 \quad (6)$$

where, A is the actual absorbance at 510 nm corresponding to ferrous ion concentration, A_1 is the absorbance of electrolysed RhB solution prepared as per modified 1,10-phenanthroline method at 510 nm, A_2 is the absorbance of electrolysed RhB solution. For finding the value of A_2 the electrolysed solution was diluted to 25 ml.

Similarly, concentration of ferric ion concentration was measured by making ferric–salicylic acid complex. To a 5 ml of 100 mg l^{-1} salicylic acid solution, 5 ml of ferric solution was added and mixed well. The produced solution has a violet colour and peaks at 525 nm as in Fig. S4.† During the calculation of ferric ion also, blank correction was carried out. The absorbance of electrolyzed RhB solution at 525 nm was reduced from the absorbance of ferric–salicylic acid complex.

C. Results and discussion

Characterisation of catalysts

Fe_3O_4 samples were prepared in laboratory by considering various Fe^{2+} : Fe^{3+} ratios such as 1 : 0, 0 : 1, 1 : 1, 2 : 1, 1 : 2, 1 : 4 and 4 : 1. The total concentration of the iron in the solution was kept constant as 0.075 M for all the combinations. With the increase in the concentration of Fe^{3+}, the color of the solution after the addition of 8 M NaOH was changed from black to brown. Moreover, the solution having 0.075 M Fe^{3+} (0 : 1 ratio) didn't give any precipitation of magnetite.

The XRD pattern of magnetite for the various ferrous–ferric ratios is presented in Fig. 1. The diffraction peaks at 30.2, 35.6, 43.2, 56.8 and 62.8°, confirms the formation of Fe_3O_4 (JCPDS file no. 89-2355) in the case of all prepared materials except for the ratio 0 : 1. In the case of 0 : 1, the peaks were obtained at 21.2; 27.2; 31.6; 33.1; 34.6; 36.6; 39.9; 41.1; 45.3; 53.1; 56.3; 58.9; 61.3; 63.9 and 66.1°, indicates the formation of NaCl (JCPDS file no. 88-2300), $NaOCl_2$ (JCPDS file no. 79-2101), FeOOH (JCPDS file no. 81-0464) and Fe_2O_3 (JCPDS file no. 85-0987). The similar peaks were also observed in the case of material with ferrous–ferric ratio of 1 : 4. This indicates that, increase in ferric ion concentration decreases the magnetite formation quantity. It was also observed from the figure that, the crystalline nature of the prepared magnetite samples was increased with increase in ferric ion concentration.

The average particle size (Table 1) of magnetite was calculated from the full width at half maximum of the peak at 35.6°, using the Debye–Scherrer formula (eqn (7))[29,30] where, D is the mean diameter of nanoparticles, β is the full width at half-maximum value of XRD diffraction lines, λ is the wavelength of X-ray radiation source 0.15405 nm, θ is the half diffraction angle -Bragg angle and K is the Scherrer constant with a value ranging from 0.9 to 1 (for the present study, the K value of 0.95 was considered). It is also observed from the Table 1 that the size of prepared material increased with increase in ferric ion concentration. In the case of magnetite prepared at the ratio of 1 : 4, the Fe^{3+} makes possible for the Fe_3O_4 formation with greater particle size without calcinations at high temperatures. Usually the particle size depends on the temperature, but in the present case the particle size was increased with concentration of Fe^{3+}.

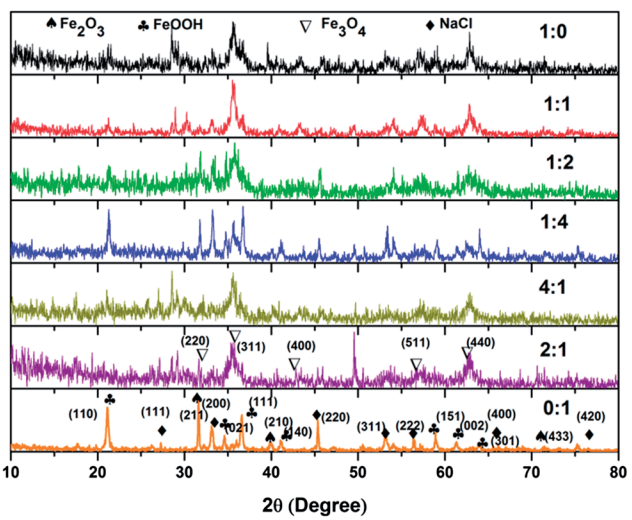

Fig. 1 XRD spectra of prepared catalysts.

Table 1 Particle size and efficiencies of prepared materials

Fe^{2+}/Fe^{3+}	Particle size (nm)	Dye removal (%)	First order rate constant (min^{-1})
1 : 0	13.6	86.79	0.016
4 : 1	14.6	86.42	0.015
2 : 1	14.5	94.09	0.019
1 : 1	18.9	88.63	0.014
1 : 2	14.2	93.22	0.018
1 : 4	31.5	89.16	0.014
0 : 1	30.9	—	—

$$D = \frac{K\lambda}{\beta \cos \theta} \quad (7)$$

The functional groups present in the magnetite were studied using FTIR and the obtained spectra are shown in Fig. 2. The presence of surface hydroxyl groups was observed by the broad absorption band presented at 3418.61 cm^{-1}.[21] This may be due to the presence of $Fe(OH)_2$, $Fe(OH)_3$, or FeOOH on the surface of Fe_3O_4, formed during the hydrolyzation process at the time of washing.[31] The presence of Fe_3O_4 was confirmed by the peaks observed at 1623.44 and 600 cm^{-1}. The intensity of the peak at 1623.44 and 600 cm^{-1} decreased with increase in ferric ion concentration, indicates the less formation of magnetite particles with increase in ferric ion concentration. The peaks at 1623.44 cm^{-1} indicated the existence of Fe–O[31] and intrinsic stretching vibrations of the metal at the tetrahedral site was observed at 600 cm^{-1}.[32]

The diffuse reluctance spectroscopy (Fig. 3) is a much acknowledged method for the identification and characterization of metal ion framework existence and its coordination. The strong absorption band observed below 300 nm in all samples is due to the ligand to metal charge transfer that involved in the isolated tetra coordinated Fe^{3+} ($t_1 \rightarrow t_2$ and $t_1 \rightarrow e$). The peak around 300–400 nm is due to Fe^{3+} and Fe^{2+} occupied at the octahedral sites. The small broadening in 400–550 nm range was consigned for the oxygen to metal charge transfer (Fe^{3+}). The larger particle size and crystallinity of 0 : 1, 1 : 4 and 4 : 1 Fe^{2+}–Fe^{3+} ratio were again confirmed by DRS UV-Vis spectra. The small shift in the absorption position for these three ratio's is due to change in the particle size of the prepared Fe_3O_4.

The SEM images of prepared catalysts at various ferrous/ferric concentrations are shown in Fig. 4. The morphology of the materials differs in the concentrations of both ferrous and ferric ions. Various morphologies were observed for all the prepared materials at different ferrous to ferric ion concentrations. Typical EDX spectrum of the prepared material is shown in Fig. S5.†

Selection of catalyst

All the prepared magnetite ratios, except 0 : 1 ratio was used for the removal of RhB from aqueous solution, as XRD analysis revealed the absence of magnetite formation. The magnetite concentration of 10 mg l^{-1} was subjected to 10 mg l^{-1} RhB solution kept in an applied voltage of 8 V. The results obtained from the kinetic removal of RhB from aqueous solution indicated that all the catalysts have higher dye removal efficiency (Fig. S6†). The removal efficiencies of various catalysts along with first order kinetic rate constants also given in Table 1. The removal efficiencies of magnetite varied from 86 to 93% after 180 min of electrolysis. Several studies indicated that magnetite with 1 : 2 ratio is the optimal combination for the maximum precipitation of Fe_3O_4 and degradation or removal of various pollutants.[21,27] In contrary to this, all the prepared magnetite followed almost the same rate of RhB removal. This is mainly due to maintaining the ferrous concentration in the solution as constant by the regeneration of Fe^{2+} at the cathode. Among the prepared materials, magnetite with 1 : 2 and 2 : 1 ratios had slightly higher removal efficiency with other combinations. Therefore, magnetite with 2 : 1 was selected for the further studies.

Effect of electrolysis time and dye concentration

The optimal concentration of iron catalyst required for EF process is very much less than the conventional Fenton process.

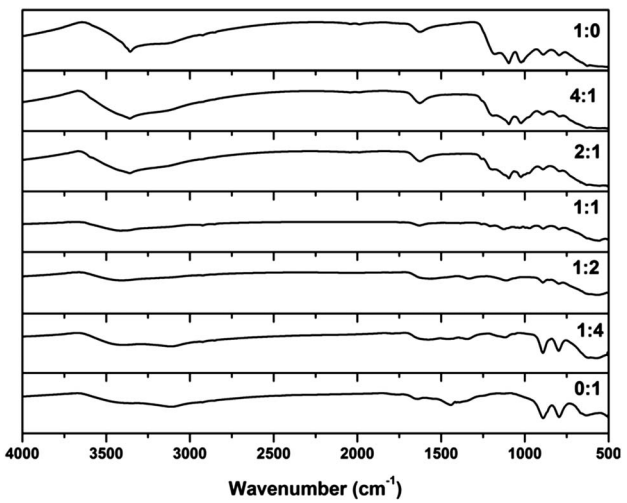

Fig. 2 FTIR spectra of prepared catalysts.

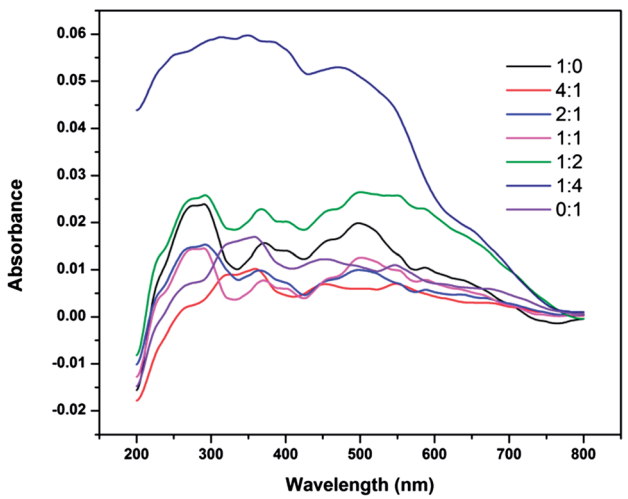

Fig. 3 DRS-UV-Visible spectra of prepared catalysts.

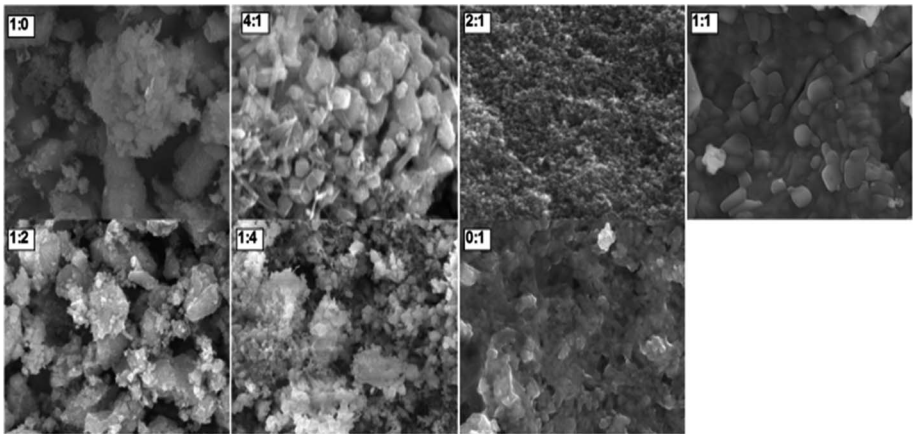

Fig. 4 SEM images of prepared catalysts.

Generally, the optimal catalyst concentration of EF process is in the range of mg l^{-1}, while that of Fenton process is g l^{-1}.[2] Our previous study[33] reported that the optimal concentration of magnetite and hydrogen peroxide required for the 86% Magenta MB removal are 600 mg l^{-1} and 0.26 M, respectively.

RhB remained in the solution during the electrolysis using magnetite as heterogeneous EF catalyst is shown in Fig. 5. The removal rate of RhB was very high at the initial stages of the electrolysis. For example, 63% of the RhB was removed within 20 min of the electrolysis. At the initial stages of electrolysis, the pores in graphite cathode were free from the contaminants. Therefore, the production of H_2O_2 and consequent hydroxyl radical production was also very high. At the initial stages, the rate of collision between hydroxyl radical and RhB molecules is very high and it will enhance the RhB removal rate. As the electrolysis time increases, the concentration of RhB reduces and that of byproducts increases. This increases the rate of collision between hydroxyl radical and byproducts than that of hydroxyl radical with RhB molecules. As the electrolysis continues the pores of the graphite cathode get occupied by various intermediates and reduce the production of H_2O_2. Özcan *et al.*[12] observed a fast electrogeneration of H_2O_2 in the first 50 min of electrolysis. But further electrolysis resulted in a decrease in the H_2O_2 accumulation rate and reached to a steady state value when its generation rate at the cathode and its decomposition rate of the anode became equal.[12] Hence, as the electrolysis time elapses the rate of RhB removal also get reduced slowly and come near to saturation.

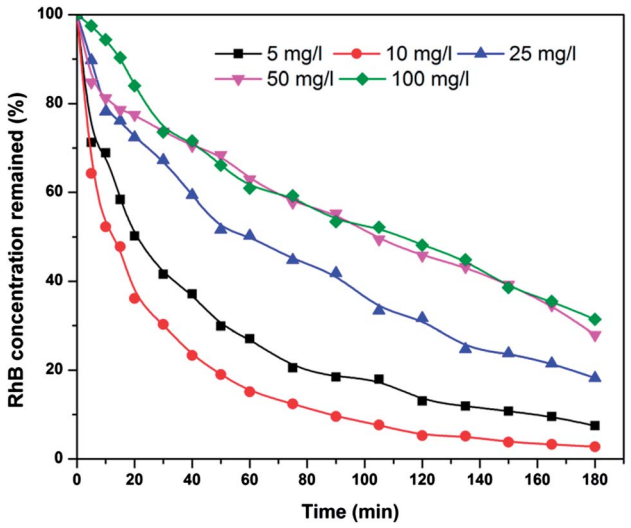

Fig. 5 Kinetic profiles of dye remained by the heterogeneous EF process at various initial RhB concentrations (Experimental conditions: catalyst concentration of 10 mg l^{-1}, applied voltage of 8 V, solution pH of 3, electrode area of 25 cm^2, inner electrode gap of 4 cm; pseudo first order kinetic constants (min^{-1}): 0.016 (5 mg l^{-1}), 0.023 (10 mg l^{-1}), 0.01 (25 mg l^{-1}), 0.007 (50 mg l^{-1}) and 0.006 (100 mg l^{-1})).

The effect of RhB concentrations on the efficiency of the heterogeneous EF process was carried out at various RhB concentrations varying from 5 to 100 mg l^{-1} (Fig. 5). With the increase of RhB concentration from 5 to 10 mg l^{-1}, the rate of RhB removal was also increased significantly. This is due to the scavenging effect of excess magnetite particles caused for 5 mg l^{-1} RhB solution. The optimal catalyst concentration required for the treatment of 5 mg l^{-1} RhB solution may be less than 10 mg l^{-1}. Excess catalysts present in the solution will produce excess Fe^{3+}, which will react with H_2O_2 to produce hydroperoxyl radicals ($HO_2^{\cdot}$) of less oxidation capability than hydroxyl radical (eqn (8)).[15,34] In addition, the excess Fe^{2+} in the solution may react with hydroxyl radical as in eqn (9) and diminish the concentration of hydroxyl radicals.[14,35–37]

$$Fe^{3+} + H_2O_2 \rightarrow FeO_2H^{2+} + H^+ \leftrightarrow HO_2^{\cdot} + Fe^{2+} + H^+ \quad (8)$$

$$Fe^{2+} + HO^{\cdot} \rightarrow Fe^{3+} + HO^- \quad (9)$$

Further increase in initial dye concentration of 10 mg l^{-1}, reduced the efficiency of the heterogeneous EF process. This may be due to the insufficient amount of hydroxyl radical produced in the system. Also, as the concentration increases the collision between hydroxyl radical also increases as explained above, which will produce more byproducts than that in lesser dye concentration. As time elapses, the rate of collision between hydroxyl radical with byproducts will increase than that of dye

molecules. Therefore, removal of dye decreases with increase in initial concentration.

Fig. S7† presents the spectral changes of RhB during electrolysis in the presence of magnetite. The RhB removal was rapid at initial stages of electrolysis with a decrease in peak at 558 nm and this rate of removal was slowed down with electrolysis time. At the same time, the absorption peaks at 295 nm increased with electrolysis time. The absorption in this region might correspond to phenol or benzene derivatives.

Wu *et al.*[38] and Wang *et al.*[39] studied the photo catalytic degradation of RhB from aqueous solution. Both study reports that de-ethylation of RhB was occurred during photo catalysis. This was verified using UV-Visible spectra also. But in electro Fenton process, the degradation occurs mainly due to the cleavage of aromatic chromophore.

The characteristic absorption peak of RhB in the solution contains two bands: the main band in the visible region has a maximum absorption at 553.8 nm and the other band in the ultraviolet region has a maximum absorption at 300 nm. The characteristic absorption peak is attributed to the dye chromophore structure.[40] The absorption peaks of RhB at 553.8 decreased with electrolytic time. This suggests that the conjugated xanthene ring in RhB is efficiently decomposed by graphite–graphite EF system.[41] There are two ways of removal of RhB; first one is the degradation of RhB by the attack of hydroxyl radical in the bulk solution, principally at the aromatic chromophore ring and the reduction of absorption without wavelength shift.[42,43] The other possible mechanism corresponds to the de-ethylation from the aromatic rings, causing a significant blue wavelength shift.[44] The color of RhB aqueous solution was turned from red to light green when the ethyl groups were fully eliminated from the solution. Consequently the wavelength of adsorption peak shifted to around 500 nm.[45] This change was not observed during the electrolysis, indicates that removal of RhB was only due to degradation process caused by hydroxyl radical oxidation.

Effect of catalyst dosage

Catalyst concentration is one of the parameters controlling the production of hydroxyl radical and efficiency of Fenton processes. Lesser and higher concentrations of catalyst will negatively affect the efficiency of EF process. As an attempt to optimize the magnetite concentration of the heterogeneous EF system, RhB removal was investigated at three initial catalyst concentration levels such as 5, 10 and 15 mg l^{-1}. The RhB removal kinetics of heterogeneous EF process as a function of magnetite concentration is shown in Fig. 6. An effective RhB removal was observed for 10 mg l^{-1} of magnetite with optimal dye removal efficiency of 97.3% after 180 min of electrolysis. Increase and decrease in the magnetite concentration from 10 mg l^{-1} decreased the efficiency of EF system. The less efficiency of the system at 5 mg l^{-1} of magnetite is mainly due to the insufficient production of hydroxyl radical in the presence of lesser iron species. In contrary to this, lesser RhB removal at higher magnetite concentration is mainly due to the scavenging reactions of excess iron species such as the production of

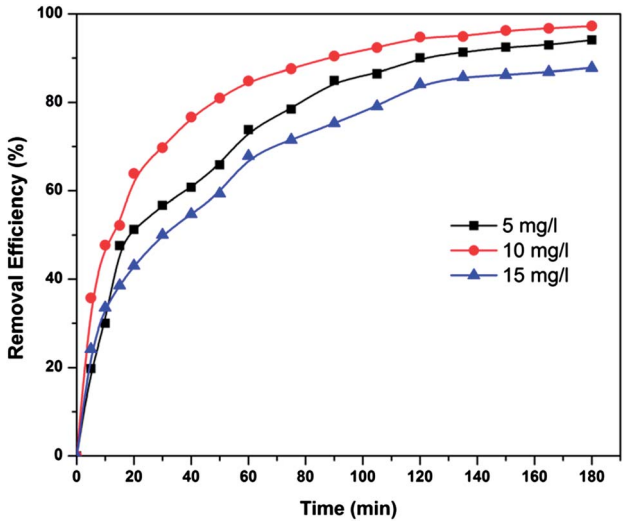

Fig. 6 Effect of Fe_3O_4 concentrations on RhB removal kinetics (Experimental conditions: applied voltage of 8 V, electrode area of 25 cm^2, electrode spacing of 4 cm and solution pH 3; pseudo first order kinetic constants (min^{-1}): 0.018 (5 mg l^{-1}), 0.023 (10 mg l^{-1}) and 0.013 (15 mg l^{-1})).

hydroperoxyl radicals and the reaction of ferrous ions with hydroxyl radical as explained above. Additionally, the active sites on the cathode surface are presumably occupied by Fe^{3+}, leading to the reduction of the number of effective sites on the cathode surface for the production hydrogen peroxide.[13] Therefore, 10 mg l^{-1} of magnetite was selected as the optimal concentration for the heterogeneous EF system and catalyst concentration for further experiments.

Increasing pH is one of the drawbacks of conventional Fenton process and is mainly due to the increase in hydroxyl ion concentration by the Fenton reactions.[1,2] In the present study an insignificant change in pH was observed, even at higher catalyst concentration. This is mainly due to the balancing of protons consumed at cathode by the water oxidation at anode.[10] Therefore the increase or decrease in solution pH in EF process is mainly depends on the degradation products. An insignificant change in pH during EF process was reported by various researchers.[10]

Effect of solution pH

The pH can affect iron solubility, complexation, and redox cycling between 2+ and 3+ states of iron.[3] Most of the studies have been reported that solution pH of 3 is the optimum condition for efficient working of Fenton processes.[16,17] In order to confirm this, electrolysis of 10 mg l^{-1} RhB solution was carried out at various solution pH values such as 2.5, 3 and 3.5 (Fig. 7). The present study also verified that the solution pH of 3 is an optimum condition for Fenton processes. Increase and decrease in solution pH from 3, decreased the efficiency of EF process. This reduction was very significant for the increase in pH from 3 to 3.5. When the solution pH increased from 3 to 3.5, RhB removal efficiency of EF process decreased from 85 to 53% after 60 min of electrolysis. Sun and Pignetallo[46] reported

that solution pH of 2.8 is the best condition for the *in situ* production of H_2O_2. In contrary to this, Özcan *et al.*[12] reported that a pH of 5 was the most suitable and optimized pH for the production of H_2O_2 generation using carbon sponge as cathode. These results indicate that, electrolytic *in situ* H_2O_2 production depends only on pH conditions and it does not have any specific optimal solution pH. Therefore, the precise optimal pH of Fenton process is related to the behaviour of Fenton catalyst. Fe^{3+} controls the iron solubility equilibrium at solution pH less than 3.5. Therefore solution having a pH less than 3.5 contains a higher concentration of Fe^{3+} and enhances the Fenton reactions. As the pH increases from 3.5, the solubility equilibrium is controlled by hydroxyl complexes of iron such as $Fe(OH)^{2+}$, $Fe(OH)_3$, $Fe(OH)_4^-$ *etc.* At these pH values, the removal of pollutant is mainly due to coagulation or sorption process.[2] This has been proven by the results reported by Modirshahla *et al.*[47] The author reported that almost constant tartrazine removal was observed after solution pH of 4 during electrocoagulation process. This trend remains constant up to a solution pH of 8. At pH values less than 3 the removal of dye was very less. At this condition, the solution contains more Fe^{3+} than hydroxyl complexes. Since hydroxyl complexes are responsible for the floc formation, an abrupt dye removal reduction was observed at pH less than 3.

At low pH values, the occurrence of two side reactions such as reduction of H_2O_2 to H_2O (eqn (10)) and production of H_2 gas (eqn (11)) will reduce the efficiency of the EF system.[12] In addition, the excess H^+ ions will react with hydroxyl radical at low pH conditions as in eqn (12).[48] Formation of oxonium ion is another scavenging reaction at lower pH values. H_2O_2 produced in the solution reacts with excess protons and forms oxonium ions as in eqn (13). $H_3O_2^+$ is electrophilic, leading to the decreasing rate of reaction between H_2O_2 and Fe^{2+}.[49,50]

$$H_2O_2 + 2H^+ + 2e^- \rightarrow 2H_2O \quad (10)$$

$$2H^+ + 2e^- \rightarrow H_2 \quad (11)$$

$$HO^{\bullet} + H^+ + e^- \rightarrow H_2O \quad (12)$$

$$H_2O_2 + H^+ \rightarrow H_3O_2^+ \quad (13)$$

Effect of applied voltage

The applied voltage is an important operational parameter affecting the efficiency of the EF process because reduction of oxygen and generation of hydrogen peroxide at cathode directly depends on applied current.[18] The RhB removal kinetics of the EF process at different voltages is shown in Fig. 8. A slight increase in dye removal efficiency of the system was observed with the increase of voltage from 6 to 8 V, which is mainly due to the increase in hydroxyl radical production rate. The current density of the system increases with increase in applied voltage, which will enhance the rate of production of H_2O_2 at the cathode.[51] The electroregeneration of Fe^{2+} from Fe^{3+} also increases with increase in current density.[19] More RhB molecules attract towards the cathode with the increase in applied voltage therefore, the collision between hydroxyl radical and dye molecules increases which will result in higher removal efficiency. But, further increase in applied voltage didn't have any significant effect on dye removal efficiency. The RhB removal efficiency of the system remains at a constant value of 97.3% after 180 min of electrolysis. Similar results were observed by Özcan *et al.*[51] for the degradation of picloram from aqueous solution. Further increase in applied voltage from 10 to 12 V, decreased the efficiency of EF process. This is due to various competitive reactions such as decomposition of H_2O_2 as in eqn (14),[19] formation of H_2O (eqn (3)),[51] and the evolution hydrogen at the cathode (eqn (11)).[19] Even though both 8 and 10 V had the

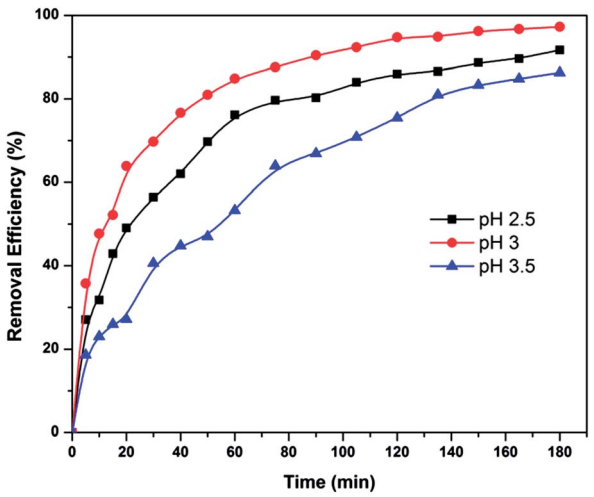

Fig. 7 RhB removal kinetics as a function of solution pH (Experimental conditions: applied voltage of 8 V, catalyst concentration of 10 mg l^{-1}, electrode area of 25 cm^2 and inner electrode spacing of 4 cm; pseudo first order kinetic constants (min^{-1}): 0.015 (pH 2.5), 0.023 (pH 3) and 0.012 (pH 3.5)).

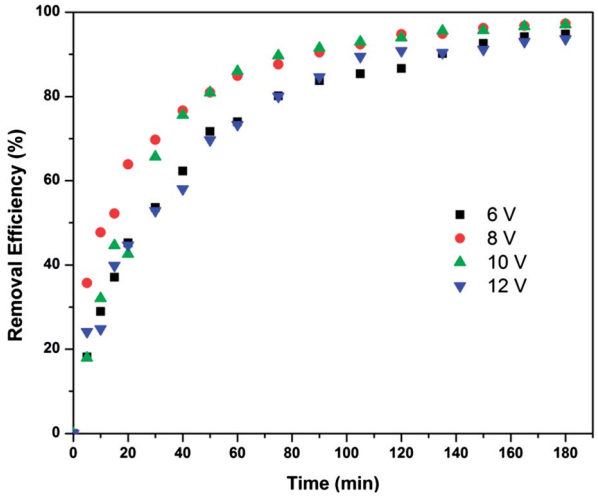

Fig. 8 Effect of applied voltage on RhB removal by heterogeneous EF process (Experimental conditions: catalyst concentration of 10 mg l^{-1}, solution pH 3, electrode area of 25 cm^2 and inner electrode spacing of 4 cm; pseudo first order kinetic constants (min^{-1}): 0.018 (6 V), 0.023 (8 V), 0.023 (10 V) and 0.018 (12 V)).

same removal efficiency, 8 V was considered as optimum and selected for the further studies due to less energy consumption.

$$2H_2O_2 \rightarrow 4H^+ + O_2 + 4e^- \quad (14)$$

Effect of inner electrode spacing

The inner electrode gap is an important parameter affecting the efficiency of all electrolytic systems. The kinetics of RhB removal as a function of inner electrode distance is shown in Fig. 9. A sharp increase in dye removal efficiency was observed; when the spacing decreased from 5 to 4 cm. Low removal efficiency at 5 cm is mainly due to the increase in ohmic drop and decrease in the mass transfer rate of Fe^{3+}.[52,53] An insignificant change in dye removal was observed for a further decrease in space from 4 to 3 cm. Similar trends were reported by Zhang *et al.*[19] for the treatment of landfill leachate by EF process. With the decrease of space from 3 to 2 cm, the efficiency of the system decreased abruptly. This is due to the oxidation of electro regenerated Fe^{2+} to Fe^{3+} at anode as in eqn (15).[19]

$$Fe^{2+} \rightarrow Fe^{3+} + e^- \quad (15)$$

Effects of anions

In order to find the effect of various anions on the RhB removal efficiency of the heterogeneous Fenton process, 5 mg l^{-1} of sodium salts containing carbonate, bicarbonate, chloride, nitrate and sulphate were added to the EF system. The above mentioned salts enhance the ionic strength and thus conductivity of the solution. Addition of these salts should increase the efficiency of EF system. El-Desoky *et al.*[10] observed a 100% removal of azo dyes in the presence of Na_2SO_4 and NaCl.

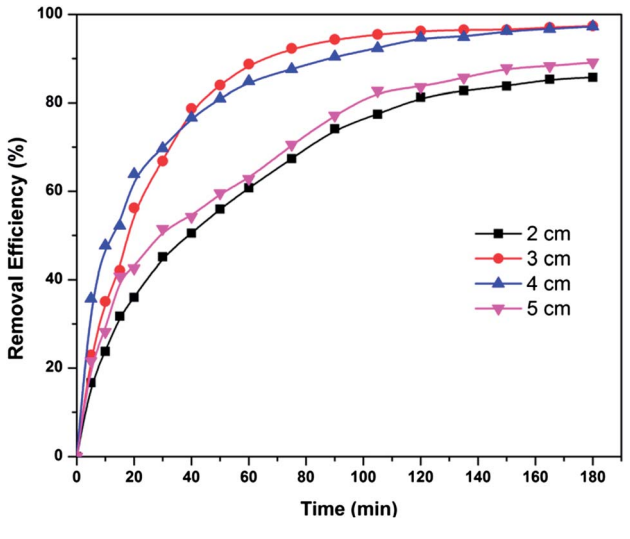

Fig. 9 Effect of inner electrode spacing on dye removal kinetics (Experimental conditions: applied voltage of 8 V, solution pH 3, electrode area of 25 cm^2 and magnetite concentration of 10 mg l^{-1}; pseudo first order kinetic constants (min^{-1}): 0.013 (2 cm), 0.024 (3 cm), 0.023 (4 cm) and 0.014 (5 cm)).

Similarly, an increase in methyl red removal from 56 to 80% was observed by Zhou *et al.*,[54] when Na_2SO_4 concentration increased from 0.05 to 0.1 M. In contrary to this, the addition of all the salts decreased the dye removal efficiency of the EF process. Percentage of dye removal along with pseudo first order rate constants of heterogeneous EF in the presence of various anions is given in Table 2. The scavenging effect of all the anions followed the order: $CO_3^{2-} \sim Cl^- > SO_4^{2-} > NO_3^- > HCO_3^-$. The scavenging effects of sulphate and nitrate are mainly due to the consumption of *in situ* produced hydroxyl radicals as shown in eqn 16 and 17 respectively.[54–58] Similarly, chloride ions act as a radical scavenger (eqn (18) and (19)) that may retard the RhB removal reaction.[59–61] Formation of $FeCO_3$ is the main dye removal retardation reaction occurs in the case of CO_3^{2-}.[62]

$$HO^\bullet + SO_4^{2-} \rightarrow HO^- + SO_4^{\bullet -} \quad (16)$$

$$HO^\bullet + NO_3^{2-} \rightarrow HO^- + NO_3^\bullet \quad (17)$$

$$HO^\bullet + Cl^- \rightarrow ClOH^{\bullet -} \quad (18)$$

$$ClOH^{\bullet -} + Cl^- \rightarrow Cl_2^{\bullet -} + OH^- \quad (19)$$

In order to find the effect of anion concentrations on RhB removal efficiency of heterogeneous EF process, electrolysis were carried out at various chloride concentration ranging from 0 to 20 mg l^{-1}, as in Fig. S8.† From the figure, it can be seen that the efficiency of the electrolytic system decreased with increase in chloride concentration. A sharp decrease in RhB removal efficiency was observed with an addition of 5 mg l^{-1} chloride into the system. But increase in chloride concentration from 10 to 20 mg l^{-1}, had an insignificant effect on the efficiency of the system. This may be due to increase in ionic strength of the solution and resulting increase in current density.

Dye removal mechanism

The schematic diagram of the RhB removal mechanism by Fe_3O_4 in an electrolytic system is shown in Fig. 10. Fe_3O_4 containing 2 : 1 ratio of Fe^{2+} and Fe^{3+} was used for the removal of RhB from aqueous solution. In acidic conditions, iron species present in the Fe_3O_4 heterogeneous catalyst get released and dissolve in the solution. At the same time, H_2O_2 was produced

Table 2 Percentage of dye removal and first order kinetic rate constants of heterogeneous EF process in the presence of anions[a]

Anions	Dye removal (%)	Rate constant (min^{-1})
Without anions	97.26	0.023
Bicarbonate	94.17	0.018
Carbonate	86.32	0.012
Chloride	86.85	0.012
Sulphate	88.26	0.013
Nitrate	93.14	0.016

[a] Experimental conditions: initial RhB concentration of 10 mg l^{-1}, solution pH 3, catalyst concentration of 10 mg l^{-1}, applied voltage of 8 V, electrode area of 25 cm^2 and inner electrode spacing of 4 cm.

at cathode by the reaction between air supplied and protons as in eqn (1). Since all the iron species releasing out from Fe_3O_4 are cationic, they are attracted towards the cathode. Fe^{2+} reacts with electrogenerated H_2O_2 and produces hydroxyl radicals. Similarly, ferric ions are reduced to ferrous ions at the cathode and follow the same. RhB is a cationic dye and is also attracted towards the cathode. Hydroxyl radicals collide on RhB molecules and oxidation reaction occurs near the cathode surface. Hence, byproducts of RhB degradation come into the solution and further degradation of byproducts also occurs in the same way as explained above.

Comparison with the homogeneous EF process

Our previous works[63,64] demonstrated that EF process is very efficient for the removal of RhB from acidic medium. Ferrous ion was used as Fenton catalyst for the removal of RhB from aqueous solution using graphite–graphite EF system. At the optimal conditions such as the applied voltage of 8 V, solution pH of 3, catalyst concentration of 10 mg l^{-1}, electrode area of 25 cm^2, and inner electrode spacing of 4 cm, 99.2% of RhB removal was obtained after 180 min of electrolysis.

Magnetite has a cubic inverse spinel structure with tetrahedral and octahedral sites filled by Fe cations.[65] The octahedral sites are occupied by both Fe^{2+} and Fe^{3+}, allowing the Fe species to be reversibly oxidized and reduced while retaining the pristine crystal structure.[65,66] In the heterogeneous EF process using Fe_3O_4, 97.3% of RhB was removed at the same conditions. This indicates that the heterogeneous EF process is also having the same efficiency for removing dyes from aqueous solution by the electrogeneration of Fenton catalysts.

Apart from this, the reusability of magnetite for the oxidation of RhB was tested under standard conditions and results obtained for five cycles are shown in Fig. 11. From the figure, it can be observed that the efficiency of magnetite remains same even after five recycles. These results indicate the possibility of using magnetite for a longer operation time.

Comparison with commercially available iron oxide

Dye removal efficiency of magnetite was compared with that of commercially available iron oxide (Fig. S9†). Magnetite had higher RhB removal efficiency and rate than that of commercially available iron oxide. In the presence of magnetite, 84.8% of RhB was removed from the aqueous solution. At the same time, 60% of RhB was removed in the presence of commercially available iron oxide.

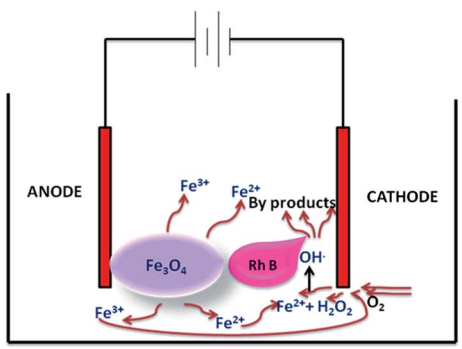

Fig. 10 RhB removal mechanism of the heterogeneous EF process using Fe_3O_4.

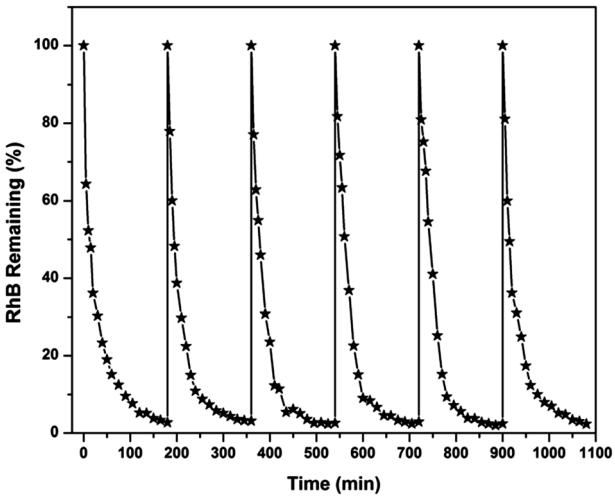

Fig. 11 RhB removal efficiencies of recycled magnetite (Experimental conditions: initial RhB concentration of 10 mg l^{-1}, solution pH 3, catalyst concentration of 10 mg l^{-1}, applied voltage of 8 V, electrode area of 25 cm^2 and inner electrode spacing of 4 cm).

Leaching of Fe ions from magnetite

The variation of ferrous and ferric ions during the electrolysis is shown in the Fig. 12. The sudden increase in ferrous and ferric ion concentrations at the initial stages of the electrolysis is mainly by the leaching of Fe ions from the magnetite. The concentration of ferrous ion increased with electrolysis time upto 30 min and then decreased with electrolysis time. The optimal concentration of ferrous ion obtained as 1.63 mg l^{-1} at 30 min of electrolysis. The decrease in ferrous ion concentration is mainly due to the Fenton oxidation process. The fluctuation in ferrous ion concentration after 30 min of electrolysis is mainly due to the regeneration of ferrous ions from ferric ions. But, the concentration of ferric ions increased with electrolysis time. This indicates that the leaching of Fe ions occurred from the magnetite as the time elapses. The optimal concentration of ferric ion (3.85 mg l^{-1}) was observed at 135 min of electrolysis. Further increase in electrolysis time reduced the ferric ion concentration due to the cathodic reduction of ferric hydroxides.

D. Conclusions

Fe_3O_4 was proved as an efficient heterogeneous electro Fenton catalyst for the removal of RhB from aqueous solution. 97.3% of RhB was removed after 180 min of electrolysis at optimal conditions from aqueous solution using graphite–graphite EF system. Optimal operational conditions of this system were found at: solution pH of 3, catalyst concentration of 10 mg l^{-1}, inner electrode spacing of 4 cm and applied voltage of 8 V. The scavenging effect of inorganic salts addition on RhB removal

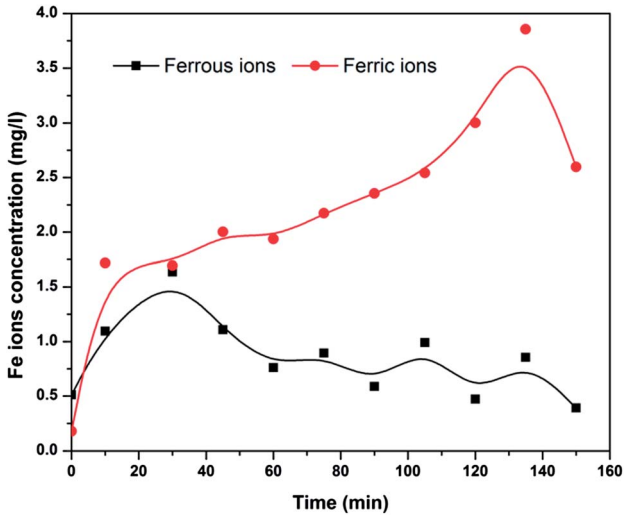

Fig. 12 Variation of ferrous and ferric ion concentrations during electrolysis (Experimental conditions: initial RhB concentration of 10 mg l^{-1}, solution pH 3, catalyst concentration of 10 mg l^{-1}, applied voltage of 8 V, electrode area of 25 cm^2 and inner electrode spacing of 4 cm).

kinetics followed the order: $CO_3^{2-} \sim Cl^- > SO_4^{2-} > NO_3^- > HCO_3^-$. Magnetite had comparable RhB removal efficiency of homogeneous EF process and had higher than that of commercially available iron oxide. From the metal leaching study, it was observed that the concentration of ferric ion in the solution was higher than that of ferrous ions at any stages of electrolysis. The optimal magnetite concentration in EF process was very much less than that of Fenton process, added additional advantage for the practical usability of this process. The reusable nature of prepared magnetite also advances the practical applicability of heterogeneous EF process over homogeneous EF process.

References

1 P. V. Nidheesh and R. Gandhimathi, *Desalination*, 2012, **299**, 1–15.
2 P. V. Nidheesh, R. Gandhimathi and S. T. Ramesh, *Environ. Sci. Pollut. Res.*, 2013, **20**, 2099–2132.
3 E. Brillas, I. Sires and M. A. Oturan, *Chem. Rev.*, 2009, **109**, 6570–6631.
4 L. Gomathi Devi, K. S. Anantha Raju and S. Girish Kumar, *J. Environ. Monit.*, 2009, **11**, 1397–1404.
5 S. Girish Kumar and L. Gomathi Devi, *J. Phys. Chem. A*, 2011, **115**, 13211–13241.
6 M. Pera-Titus, V. Garćıa-Molina, M. A. Baños, J. Giménez and S. Esplugas, *Appl. Catal., B*, 2004, **47**, 219–256.
7 B. Boye, M. M. Dieng and E. Brillas, *Electrochim. Acta*, 2003, **48**, 781–790.
8 N. Daneshvar, S. Aber, V. Vatanpour and M. H. Rasoulifard, *J. Electroanal. Chem.*, 2008, **615**, 165–174.
9 M. Zarei, D. Salari, A. Niaei and A. Khataee, *Electrochim. Acta*, 2009, **54**, 6651–6660.
10 H. S. El-Desoky, M. M. Ghoneim, R. El-Sheikh and N. M. Zidan, *J. Hazard. Mater.*, 2010, **175**, 858–865.
11 W. S. Chen and S. Z. Lin, *J. Hazard. Mater.*, 2009, **168**, 1562–1568.
12 A. Özcan, Y. Sahin, A. Savas Koparal and M. A. Oturan, *J. Electroanal. Chem.*, 2008, **616**, 71–78.
13 C. T. Wang, W. L. Chou, M. H. Chung and Y. M. Kuo, *Desalination*, 2010, **253**, 129–134.
14 M. Perez, F. Torrades, J. A. Garcia-Hortal, X. Domenech and J. Peral, *Appl. Catal., B*, 2002, **36**, 63–74.
15 M. A. Oturan, N. Oturan, M. C. Edelahi, F. I. Podvorica and K. El Kacemi, *Chem. Eng. J.*, 2011, **171**, 127–135.
16 A. L. Estrada, Y.-Y. Li and A. Wang, *J. Hazard. Mater.*, 2012, **227–228**, 41–48.
17 M. Zhou, Q. Tan, Q. Wang, Y. Jiao, N. Oturan and M. A. Oturan, *J. Hazard. Mater.*, 2012, **215–216**, 287–293.
18 T. S. N. Sankara Narayanan, G. Magesh and N. Rajendran, *Fresenius Environ. Bull.*, 2003, **12**(7), 776–780.
19 H. Zhang, D. Zhang and J. Zhou, *J. Hazard. Mater.*, 2006, **B135**, 106–111.
20 S. Zhang, X. Zhao, H. Niu, Y. Shi, Y. Cai and G. Jiang, *J. Hazard. Mater.*, 2009, **167**, 560–566.
21 G. Absalan, M. Asadi, S. Kamran, L. Sheikhian and D. M. Goltz, *J. Hazard. Mater.*, 2011, **192**, 476–484.
22 J. Deng, X. Wen and Q. Wang, *Mater. Res. Bull.*, 2012, **47**, 3369–3376.
23 L. Xu and J. Wang, *Environ. Sci. Technol.*, 2012, **46**, 10145–10153.
24 H. Niu, D. Zhang, S. Zhang, X. Zhang, Z. Meng and Y. Cai, *J. Hazard. Mater.*, 2011, **190**, 559–565.
25 J. Chun, H. Lee, S.-H. Lee, S.-W. Hong, J. Lee, C. Lee and J. Lee, *Chemosphere*, 2012, **89**, 1230–1237.
26 X. Liang, Y. Zhong, S. Zhu, J. Zhu, P. Yuan, H. He and J. Zhang, *J. Hazard. Mater.*, 2010, **181**, 112–120.
27 D. K. Kim, Y. Zhang, W. Voit, K. V. Rao and M. Muhammed, *J. Magn. Magn. Mater.*, 2001, **225**, 30–36.
28 H. Tamura, K. Goto, T. Yotsuyanagi and M. Nagayama, *Talanta*, 1974, **21**, 314–318.
29 Y. Zhu and Q. Wu, *J. Nanopart. Res.*, 1999, **1**, 393–396.
30 A. M. Awwad and N. M. Salem, *Nanosci. Nanotechnol.*, 2012, **2**(6), 208–213.
31 L. Xiaojuan, J. Guoyuan, Z. Liping, Y. Yuxiang and L. Xiangnong, *Glass Phys. Chem.*, 2011, **37**(4), 459–465.
32 E. Karaoglu, A. Baykal, H. Deligöz, M. Senel, H. Sözeri and M. S. Toprak, *J. Alloys Compd.*, 2011, **509**, 8460–8468.
33 S. Xavier, R. Gandhimathi, P. V. Nidheesh and S. T. Ramesh, *Desalin. Water Treat.*, 2013, DOI: 10.1080/19443994.2013.844083.
34 A. Özcan, M. A. Oturan, N. Oturan and Y. Şahin, *J. Hazard. Mater.*, 2009, **163**, 1213–1220.
35 M. Panizza and G. Cerisola, *Water Res.*, 2001, **35**, 3987–3992.
36 L. Gomathi Devi, S. Girish Kumar, K. Mohan Reddy and C. Munikrishnappa, *J. Hazard. Mater.*, 2009, **164**, 459–467.
37 L. Gomathi Devi, S. Girish Kumar and K. Mohan Reddy, *Cent. Eur. J. Chem.*, 2009, **7**, 468–477.
38 T. Wu, G. Liu, J. Zhao, H. Hidaka and N. Serpone, *J. Phys. Chem. B*, 1998, **102**, 5845–5851.

39 Q. Wang, C. Chen, D. Zhao, W. Ma and J. Zhao, *Langmuir*, 2008, **24**, 7338–7345.
40 B. Cuiping, X. Xianfeng, G. Wenqi, F. Dexin, X. Mo, G. Zhongxue and X. Nian, *Desalination*, 2011, **278**, 84–90.
41 C. Guo, J. Xu, Y. He, Y. Zhang and Y. Wang, *Appl. Surf. Sci.*, 2011, **257**, 3798–3803.
42 T. Watanabe, T. Takizawa and K. Honda, *J. Phys. Chem.*, 1977, **81**, 1845–1851.
43 C. Chen, W. Zhao, J. Li, J. Zhao, H. Hidaka and N. Serpone, *Environ. Sci. Technol.*, 2002, **36**, 3604–3611.
44 A. Martinez-de la Cruz, S. M. G. Marcos Villarreala, L. M. Torres-Martinez, E. Lopez Cuellar and U. Ortiz Mendez, *Mater. Chem. Phys.*, 2008, **112**, 679–685.
45 X. Chang, M. A. Gondal, A. A. Al-Saadi, M. A. Ali, H. Shen, Q. Zhou, J. Zhang, M. Du, Y. Liu and G. Ji, *J. Colloid Interface Sci.*, 2012, **377**, 291–298.
46 Y. Sun and J. J. Pignetallo, *Environ. Sci. Technol.*, 1993, **27**, 304–310.
47 N. Modirshahla, M. A. Behnajady and S. Kooshaiian, *Dyes Pigm.*, 2007, **74**, 249–257.
48 W. Z. Tang and C. P. Huang, *Environ. Technol.*, 1996, **17**, 1371–1378.
49 X. Han and D. Xia, *Sulphur Phosphorus & Bulk Materials Handling Related Engineering.*, 2004, **6**, 25–28.
50 L. Gomathi Devi, K. E. Rajashekhar, K. S. Anantha Raju and S. Girish Kumar, *J. Mol. Catal. A: Chem.*, 2009, **314**, 88–94.
51 A. Özcan, Y. Sahin, A. Savas Koparal and M. A. Oturan, *J. Hazard. Mater.*, 2008, **153**, 718–727.
52 E. Fockedey and A. V. Lierde, *Water Res.*, 2002, **36**(16), 4169–4175.
53 Z. M. Qiang, J. H. Chang and C. P. Huang, *Water Res.*, 2003, **37**, 1308–1319.
54 M. Zhou, Q. Yu, L. Lei and G. Barton, *Sep. Purif. Technol.*, 2007, **57**, 380–387.
55 L. Gomathi Devi, K. S. Anantha Raju, S. Girish Kumar and K. Eraiah Rajashekhar, *J. Taiwan Inst. Chem. Eng.*, 2011, **42**, 341–349.
56 A. Riga, K. Soutsas, K. Ntampegliotis, V. Karayannis and G. Papapolymerou, *Desalination*, 2007, **211**, 72–86.
57 L. Gomathi Devi, S. Girish Kumar, K. Mohan Reddy and C. Munikrishnappa, *Desalin. Water Treat.*, 2009, **4**, 294–305.
58 G. L. Truong, J. D. Laat and B. Legube, *Water Res.*, 2004, **38**, 2384–2394.
59 M. Abdullah, G. K.-C. Low and R. W. Matthews, *J. Phys. Chem.*, 1990, **94**, 6820–6825.
60 K. H. Wang, Y. H. Hsieh, M. Y. Chou and C. Y. Chang, *Appl. Catal., B*, 1999, **21**, 1–8.
61 M. Zhang, T. An, X. Hu, C. Wang, G. Sheng and J. Fu, *Appl. Catal., A*, 2004, **260**, 215–222.
62 D. J. Whebi, H. M. Hafez, M. H. El Masri and M. M. El Jamal, *J. Univ. Chem. Technol. Metall.*, 2010, **45**(3), 303–312.
63 P. V. Nidheesh and R. Gandhimathi, *Desalin. Water Treat.*, 2013, DOI: 10.1080/19443994.2013.790321.
64 P. V. Nidheesh and R. Gandhimathi, *Clean: Soil, Air, Water*, 2013, DOI: 10.1002/clen.201300093.
65 X. Liang, Z. He, Y. Zhong, W. Tan, H. He, P. Yuan, J. Zhu and J. Zhang, *Colloids Surf., A*, 2013, **435**, 28–35.
66 R. C. C. Costa, M. Lelis, L. Oliveira, J. Fabris, J. Ardisson, R. Rios, C. Silva and R. Lago, *J. Hazard. Mater.*, 2006, **129**, 171–178.

